NIH Public Access
Author Manuscript
Curr Opin Struct Biol. Author manuscript; available in PMC 2009 October 1.

Published in final edited form as:
Curr Opin Struct Biol. 2008 October ; 18(5): 593–600. doi:10.1016/j.sbi.2008.06.009.

Neutron crystallography:

opportunities, challenges, and limitations

Matthew P Blakeley[1], **Paul Langan**[2,3], **Nobuo Niimura**[4], and **Alberto Podjarny**[5]

1*ILL, 6 Rue Jules Horowitz, BP 156, 38042 Grenoble, France*

2*M888, Bioscience Division, Los Alamos National Laboratory, Los Alamos, NM 87545, USA*

3*Department of Chemistry, University of Toledo, Toledo, OH 53606, USA*

4*Institute of Applied Beam Science, Graduate School of Science and Engineering, Ibaraki University, 4-12-1 Naka-Narusawa, Hitachi, Ibaraki 316-8511, Japan*

5*IGBMC, 1 Rue Laurent Fries, 67404 Strasbourg-Illkirch, France*

Abstract

Neutron crystallography has had an important, but relatively small role in structural biology over the years. In this review of recently determined neutron structures, a theme emerges of a field currently expanding beyond its traditional boundaries, to address larger and more complex problems, with smaller samples and shorter data collection times, and employing more sophisticated structure determination and refinement methods. The origin of this transformation can be found in a number of advances including first, the development of neutron image-plates and quasi-Laue methods at nuclear reactor neutron sources and the development of time-of-flight Laue methods and electronic detectors at spallation neutron sources; second, new facilities and methods for sample perdeuteration and crystallization; third, new approaches and computational tools for structure determination.

Introduction

Knowing exactly where hydrogen (H) atoms are and how they are transferred between biomacromolecules, solvent molecules, and substrates is important for understanding many biological processes. Neutron crystallography (NC) is a powerful technique for locating H atoms and is used to provide information on the protonation states of amino acid residues, the identity of solvent molecules, and the nature of bonds involving H, as illustrated in Figure 1 and as recently reviewed [1]. NC can also be used to identify H atoms that are exchanged with deuterium (D) and the extent of this replacement, thus providing a tool for identifying isotopically labeled structural features and for studying solvent accessibility and macromolecular dynamics, complementary to NMR techniques. The big disadvantage of NC is the relatively low flux of available neutron beams, which requires either big crystals or very long exposure times for smaller crystals in order to have a measurable diffraction signal.

Previous reviews in this journal have outlined the advantages of using NC, but with relatively few examples of its application, and they have looked toward a brighter future in which the disadvantage of the relatively low flux of available neutron beams is overcome [2,3]. Since then there has been greatly increased activity in this field and the focus of this review is on the increasing number of new neutron structures published over the past two years. We shall

Corresponding author: Blakeley, Matthew P (blakeleym@ill.fr), Langan, Paul (langan_paul@lanl.gov), Niimura, Nobuo (niimura@mx.ibaraki.ac.jp) and Podjarny, Alberto (podjarny@titus.u-strasbg.fr).

NIH-PA Author Manuscript
NIH-PA Author Manuscript
NIH-PA Author Manuscript

NIH-PA Author Manuscript

NIH-PA Author Manuscript

NIH-PA Author Manuscript

discuss the methodological and technological advances that are responsible for this increase in scientific productivity and what opportunities, challenges, and limitations the future holds.

New structures

Details of recently published structures are given in Table 1. Combining NC of enzymes human aldose reductase (hAR) [4••,5], D-xylose isomerase (XI) from *Streptomyces rubiginosus* [6••, 7,8••], diisopropyl fluorophosphatase (DFPase) from *Loligo vulgaris* [9•], and endothiapepsin from *Endothia parasitica* [10,11] with complementary information from X-ray crystallography (XC), and quantum mechanical and molecular dynamics modeling, has answered key questions about reaction mechanisms. hAR reduces a wide range of substrates by hydride transfer from C4 of a NADPH cofactor and a proton donation from hAR itself. Blakeley *et al*. [4••] have unveiled the internal organization and mobility of the H-bond network of the catalytic engine. The results suggest that hAR overcomes the difficulty of simultaneously satisfying the requirements of being an effective catalyst and a promiscuous one by using a distal proton donor (Asp43—Lys77 pair, see Figure 2) acting on a flexible final proton carrier (Tyr48), capable of accommodating different substrates.

Two catalytic Asp-Thr-Gly sequences form the active site of the aspartic proteinase endothiapepsin, with a catalytic water bound tightly between the aspartates. Tuan *et al*. [10] and Coates *et al*. [11] have determined the H-bond arrangement in the tetrahedral binding motif formed by these aspartates and a difluoroketone (*gem*-diol) inhibitor (Figure 1a). This complex is a more complete analog of the transition state than a previous one with a hydroxyethylene inhibitor [12], and provides a snapshot of possible proton transfer during the reaction.

H atoms have been located at different stages of the sugar isomerization reaction catalyzed by XI, greatly impacting our understanding of the reaction mechanism [6••,7,8••]. After a ring-opening stage involving the His54—Asp57 pair, the substrate (xylose or glucose) is extended and tethered at either end by H bonds. A metal bound water molecule, close to the C1—C2 site of isomerization, is deprotonated as Lys289 is protonated. Meanwhile, O2 of the substrate is deprotonated and the resulting unstable intermediate is stabilized by removing H from C2 and adding H to C1. The precise role of the activated water molecule in this proton transfer remains to be determined.

Proposed catalytic mechanisms for the phosphotriesterase DFPase include esterase hydrolysis by nucleophilic attack on the phosphorus atom of the bound substrate by an activated water molecule. However, the recent observation of a covalent intermediate between substrate and Asp229 suggests a new mechanism in which the carboxylate carbon atom of the intermediate is attacked by water [13]. Blum *et al*. have revealed that, in the holoenzyme, the catalytic calcium coordinates a key water molecule and that Asp229 is clearly deprotonated, in support of the newly proposed mechanism ([9•], MM Blum *et al*.,in preparation).

Dihydrofolate reductase (DHFR) has become an important chemotherapeutic and antimicrobial drug target. Bennett *et al.* [14••] directly revealed that a ring nitrogen atom (N1) of the anticancer drug MTX undergoes induced protonation on binding to DHFR from *E. coli*, imparting it with a favorable positive charge for ionic interaction with unprotonated Asp27, and partly explaining its preferential binding over the natural DHF substrate.

The functional mechanisms of photoactive yellow protein (PYP) from *Halorhodospira halophila* [15•] and human hemoglobin (HbA) [16••,17] have been studied by a combination of NC and XC. PYP absorbs light via its *para*-coumaric acid chromophore (pCA), covalently attached to Cys69, and is thought to be involved in the negative phototactic response of the organism to blue light. In its ground state, Fisher *et al*. [15•] have revealed that the phenolate oxygen of pCA accepts two short H bonds (from Glu46 $O^{\varepsilon 2}$ and Tyr42 O^{η}) and that Thr50

NIH-PA Author Manuscript

NIH-PA Author Manuscript

NIH-PA Author Manuscript

$O^{\gamma 1}$ stabilizes this arrangement by donating an H bond to Tyr42 O^{η}. However, D/H between pCA and Tyr42 is only partially occupied indicating a resistance to exchange or that it also interacts with Thr50, possibly in a resonance between the two bonds. HbA efficiently transports O_2 from lung to tissue. Binding of O_2 to HbA's heme sites is regulated by protons and by inorganic anions. Chatake *et al*. [16••] have determined the protonation states of key distal residues Hisα58 and Hisβ63 in the deoxy form, which contribute to the T-state Bohr effect of HbA.

Further NC data sets having been collected from biomacromolecules, including high-resolution deoxyhemoglobin [17], porcine pancreatic elastase [18], nucleic acids [19], thaumatin [20], and rasburicase [21], and structure determinations are under way.

Advances in neutron beam line technology and methods

A number of technological and methodological advances are now fully exploited on neutron beam lines. Neutron image-plates mounted on cylindrical drums, originally developed by the Japanese Atomic Energy Agency (JAEA) in the 1990s, can completely surround the sample, maximizing the number of reflections simultaneously recorded on beam lines at nuclear reactor neutron sources run by JAEA and the Institut Laue-Langevin (ILL). On BIX-3 and BIX-4 at JAEA [22,23] a series of elastically bent perfect Si plates produced a high-flux beam for monochromatic data collection with high signal-to-noise ratios. Data are collected using a step-scan mode (typically 0.3°), with each exposure lasting for 15–60 min, and a total of 500–1000 of such frames are required for a typical data set.

On LADI-III at the ILL, data are collected using a quasi-Laue method in order to provide a rapid survey of reciprocal space while reducing background scattering and reflection overlap compared to the use of the full white beam. Various Ni/Ti multilayer band-pass filters are available ($\delta\lambda/\lambda$ from 5 to 25%) so one can select the wavelength range and wavelength best suited to the sample. The crystal is mounted on a goniometer head along the cylindrical drum axis and is rotated around this axis (typically by 7°) for each successive image. The neutron beam, which enters and leaves via opposed holes in the cylinder, interacts with the crystal to produce Bragg reflections which are recorded on the neutron image-plates mounted on the inside cylindrical surface. LADI-III is a recent replacement (March 2007) for the old LADI instrument used to collect data from crystals as small as 0.15 mm^3. An improved reading system located internally provides a twofold to threefold gain in neutron detection [24]. For example, data sets have been collected in 3.5 days to 2.0Å resolution from a 1.4 mm^3 thaumatin crystal [19] and over several days to 2Å resolution from a perdeuterated antifreeze protein (AFP) only 0.13 mm^3 in volume (I Haertlein *et al*., unpublished).

The Protein Crystallography Station (PCS) at Los Alamos Neutron Science Center (LANSCE) is the first NC beam line to be built at a spallation source [25,26] and has been operational since the end of 2002. Neutrons are produced from a coupled high-flux water moderator in pulses at a rate of 20 Hz and then travel 28 m down a vacuum pipe with collimation inserts tapering the beam to a final divergence of 0.12°. The time and energy structure of the beam, and also its relatively small divergence, has allowed data to be collected efficiently and with enhanced signal-to-noise with time-of-flight (TOF) Laue techniques from crystals as small as 0.3 mm^3. The data are recorded as 3D TOF Laue patterns on a large position sensitive electronic detector with a spatial resolution of less than a millimeter, and are processed using a version of the software d*TREK modified for TOF Laue techniques [27]. This wavelength-resolved Laue technique has rapid and efficient coverage of reciprocal space and does not suffer from reflection overlap and a build up of background scattering over the selected wavelength range.

NIH-PA Author Manuscript

NIH-PA Author Manuscript

NIH-PA Author Manuscript

Advances in sample preparation

Deuteration, replacing H by D, is a powerful method for changing the scattering contrast of specific parts of a macromolecule and also for enhancing its scattering properties. Water and labile H atoms in proteins can be substituted by soaking crystals in D_2O mother liquor. To substitute the remaining H atoms (perdeuteration) requires gene expression in a deuterated growth media, which offers several advantages, such as the use of smaller crystal volumes, the ability to collect data from larger and more complex systems, shorter data collection times, and potentially higher resolution data. The ILL-EMBL Deuteration Laboratory (D-Lab), running since 2003, has allowed NC studies using crystals as small as ~0.1 mm^3 [4••,5]. At the Biological Deuteration Laboratory (BDL) at LANSCE, an algae-based approach is used, described in its application to studying the catalytic mechanism of haloalkane dehalogenase from *Xanthobacter autrophicus* by Liu *et al*. [28].

For hydrogenated proteins, optimizing crystal volume is still a bottleneck. In such situations, larger hydrogenated crystals (grown or soaked in D_2O) are required. A similar problem occurs if perdeuterated crystals are too small. Knowledge of the macromolecular crystallization phase diagram allows large crystals to be obtained. At the ILL/EMBL-Grenoble, a device which combines the use of temperature control with seeding to drive the process of crystallization has been developed [21,29]. While at JAERI, a device based on a novel dialysis method is used to grow large crystals based on the phase diagram for the protein concentration versus precipitant concentration [30-33].

Advances in structure determination and refinement methods

A Macromolecular Neutron Crystallography (MNC) consortium between Los Alamos and Berkeley National Laboratories has been established to develop computational tools (see http://mnc.lanl.gov). A patch, designated *nCNS*, for the existing structure solution program called *CNS* [34] has been developed which combines, for the first time, global XC, NC, and energy refinement with crossvalidated maximum-likelihood simulated annealing refinement. *nCNS* has already been used to determine the joint X-ray and neutron (XN) structures of PYP [15•], DFPase [9•], nucleic acids [19], endothiapepsin/difluoroketone [10], and Hba [17]. MNC has also added NC capabilities to *PHENIX* (website) and *phenix.refine* has been used to determine the XN structure of hAR [4••]. The future development of *nCNS* and *PHENIX* will be greatly aided by a ‘Hydrogen and Hydration in Proteins’ Data Base (HHDB) (http://hhdb01.tokai-sc.jaea.go.jp/HHDB/) that catalogs all H atom positions determined by NC. The HHDB is an important new research tool that provides a graphic interface for visualizing and analyzing all types of interactions involving H atoms. In addition to determining H positions, NC coupled with the H/D-exchange (HDX) method is a powerful probe for investigating molecular dynamics. A global analysis of HDX has shown that it can also be used to identify the constituents of the hydrophobic protein core and constitute minimal folding domains [35].

Hauptman and Langs have extended the neutron Shake-and-Bake (*SnB*) protocol for neutron macromolecular structure determination, by including the analysis and treatment of H/D-labeled isomorphous pairs of macromolecular structures. The first proof-of-principle experiments for these *ab initio* phasing techniques were performed on LADI-III using rubredoxin (*Pyrococcus furiosus*). Data sets were collected on both a perdeuterated rubredoxin crystal (DAA Myles *et al*., unpublished) and an ‘isomorphous derivative’, in which H-labeled amino acids, clearly seen in preliminary maps, were selectively introduced into deuterated rubredoxin [36•].

NIH-PA Author Manuscript

NIH-PA Author Manuscript

NIH-PA Author Manuscript

Conclusions

As described in the 'New Structures' section, NC has recently provided key biological information, notably about enzymatic mechanisms. This increase in the biological impact of NC is due both to the improvement of data collection facilities and of perdeuterated samples. Efforts in increasing crystal volume, still an important bottleneck, are essential to take full advantage of perdeuteration. Moreover, selective labeling of specific amino acids or nucleotides within a molecule can also allow novel approaches in structure determination [37].

The rate of expansion of NC is likely to increase with continued improvements to existing beam lines, like the recent replacement of the LADI station at the ILL by the LADI-III, and the addition of a number of new beam lines with greatly increased capabilities [38]. In addition to two new beam lines for NC at the reactor sources run by ANSTO and FRM-II, three new beam lines are being built at the next generation spallation neutron sources: the Spallation Neutron Source (SNS) at Oak Ridge National Laboratory and the Japan Proton Accelerator Research Complex (J-PARC) in Japan.

At the SNS, TOPAZ will be able to resolve unit cell edges of up to 50Å, whereas MaNDi is optimized for larger unit cell systems of 150Å and beyond [39]. At J-PARC, iBIX, scheduled for operation in 2008, is projected to improve data collection efficiency over BIX-3 and BIX-4 by two orders of magnitude [33,40]. If intensities can be increased by an order of magnitude or two, then in principle it will be possible to study crystals that are correspondingly smaller in volume. The consequences of this development will be enormous; the dramatic decrease in crystal size will have very positive impact on the usefulness of single-crystal neutron diffraction in the field of structural biology. Table 2 shows a comparison between different neutron sources, present and future.

Acknowledgements

PL was supported by grants from the National Institute of General Medical Science of the National Institutes of Health (1R01GM071939-01), LANL LDRD (20070131ER and 20080001DR), and by the Office of Biological and Environmental Research of the Department of Energy. ADP was supported by the Human Frontiers Science Program, by the Centre National de la Recherche Scientifique (CNRS), by the Institut National de la Santé et de la Recherche Médicale, and the Hêpital Universitaire de Strasbourg (H.U.S). NN was supported partly by a Grant-in-Aid for Scientific Research from the MEXT of Japan. NN and ADP were supported by the Human Frontiers Science Program (RGP0021/2006-C). The construction of the LADI-III diffractometer was financed by a grant from the European Commission (Grant No. 011995 CISB (RICN)).

References and recommended reading

Papers of particular interest, published within the period of review, have been highlighted as:

• of special interest

• • of outstanding interest

1. Niimura N, Bau R. Neutron protein crystallography: beyond the folding structure of biological macromolecules. Acta Cryst A 2008;64:12–22. [PubMed: 18156668]

2. Niimura N. Neutrons expand the field of structural biology. Curr Opin Struct Biol 1999;9(5):602–608. [PubMed: 10508767]

3. Myles DAA. Neutron protein crystallography: current status and a brighter future. Curr Opin Struct Biol 2006;16:630–637. [PubMed: 16963258]

4 ••. Blakeley MP, Ruiz F, Cachau R, Hazemann I, Meilleur F, Mitschler A, Ginell S, Afonine P, Ventura ON, Cousido-Siah A, et al. Quantum model of catalysis based on a mobile proton revealed by subatomic x-ray and neutron diffraction studies of h-aldose reductase. Proc Natl Acad Sci U S A

NIH-PA Author Manuscript

NIH-PA Author Manuscript

NIH-PA Author Manuscript

2008;105(6):1844–1848. [PubMed: 18250329]The combination of neutron and subatomic resolution X-ray crystallography of a complex of deuterated h-aldose reductase with an inhibitor showed the mobility of a proton in an Asp—Lys pair, which was essential to propose a new model of catalysis. Neutron diffraction was collected with a crystal radically smaller (0.15 mm^3) than the usual size, showing the importance of full deuteration.

5. Blakeley MP, Mitschler A, Hazemann I, Meilleur F, Myles DAA, Podjarny A. Comparison of hydrogen determination with X-ray and neutron crystallography in a human aldose reductase— inhibitor complex. Eur Biophys J 2006;35:577–583. [PubMed: 16622654]

6 ••. Katz AK, Li X, Carrell HL, Hanson BL, Langan P, Coates L, Schoenborn BP, Glusker JP, Bunick GJ. Locating active-site hydrogen atoms in D-xylose isomerase: time-of-flight neutron diffraction. Proc Natl Acad Sci U S A 2006;103(22):8342–8347. [PubMed: 16707576]A combination of TOF neutron Laue data (1.8Å) and high-resolution X-ray data (0.94Å) collected from native D-xylose isomerase is used to reveal the location of active-site hydrogen atoms and to contribute to the elucidation of the enzyme's mechanism.

7. Meilleur F, Snell EH, van der Woerd MJ, Judge RA, Myles DAA. A quasi-Laue neutron crystallographic study of D-xylose isomerase. Eur Biophys J 2006;35:601–609. [PubMed: 16673077]

8 ••. Kovalevsky AY, Katz AK, Carrell HL, Hanson L, Mustyakimov M, Fisher SZ, Coates L, Schoenborn BP, Bunick GJ, Glusker JP, Langan P. Hydrogen location in stages of an enzyme catalyzed reaction: time-of-flight neutron structure of D-xylose isomerase with bound D-xylulose. Biochem Rapid Rep 2008;47(29):7595–7597.The neutron structure of D-xylose isomerase with bound perdeuterated product D-xylulose, together with the neutron structure of the native enzyme, provides the location of hydrogen atoms at different stages of the enzyme-catalyzed sugar isomerization reaction, greatly impacting our understanding of the reaction mechanism.

9 •. Blum MM, Koglin A, Rüterjans H, Schoenborn B, Langan P, Chen JC. Preliminary time-of-flight neutron diffraction study on diisopropyl fluorophosphatase (DFPase) from *Loligo vulgaris*. Acta Cryst F 2007;63:42–45.DFPase, at 35 kDa, is one of the larger proteins and asymmetric units (77 626Å3) to be studied using neutron crystallography, though the crystal size used in this study is among the smallest (0.43 mm^3). This paper contains a useful practical guide to sample-size and asymmetric unit limitations for neutron structures.

10. Tuan HF, Erskine P, Langan P, Cooper J, Coates L. Preliminary neutron and ultrahigh-resolution X-ray diffraction studies of the aspartic proteinase endothiapepsin cocrystallized with a gem-diol inhibitor. Acta Cryst F 2007;63:1080–1083.

11. Coates L, Tuan HF, Tomanicek S, Kovalevsky A, Mustyakimov M, Erskine PT, Cooper J. The catalytic mechanism of an aspartic aroteinase axplored with neutron and X-ray diffraction. J Am Chem Soc 2008;130:7235–7237. [PubMed: 18479128]

12. Coates L, Erskine PT, Mall S, Gill R, Wood SP, Myles DAA, Cooper JB. X-ray, neutron and NMR studies of the catalytic mechanism of aspartic proteinases. Eur Biophys J 2006;35:559–566. [PubMed: 16673078]

13. Blum MM, Lohr F, Richardt A, Ruterjans H, Chen JCH. Binding of a designed substrate analogue to diisopropyl fluorophosphatase: implications for the phosphotriesterase mechanism. J Am Chem Soc 2006;128:12750–12757. [PubMed: 17002369]

14 ••. Bennett B, Langan P, Coates L, Mustyakimov M, Schoenborn B, Howell EE, Dealwis C. Neutron diffraction studies of *Escherichia coli* dihydrofolate reductase complexed with methotrexate. Proc Natl Acad Sci U S A 2006;103(49):18493–18498. [PubMed: 17130456]This study of DHFR in complex with the chemotherapeutic agent, methotrexate provides one of the first examples of using spallation neutrons to study protein dynamics, to identify protonation states directly from neutron density maps, and to analyze solvent structure. Using 2.2Å resolution TOF neutron Laue data collected from a 0.3 mm^3 crystal the N1 atom of methotrexate is shown to be protonated and thus charged when bound to DHFR.

15 •. Fisher SZ, Anderson S, Henning R, Moffat K, Langan P, Thiyagarajan P, Schultz AJ. Neutron and X-ray structural studies of short hydrogen bonds in photoactive yellow protein (PYP). Acta Cryst D 2007;63:1178–1184. [PubMed: 18007033]The first recent application of joint X-ray (1Å) and neutron (2.5Å) structure refinement in combination with crossvalidated maximum-likelihood simulation annealing using the program nCNS (see http://mnc.lanl.gov).

NIH-PA Author Manuscript

NIH-PA Author Manuscript

NIH-PA Author Manuscript

16 ••. Chatake T, Shibayama N, Park SY, Kurihara K, Tamada T, Tanaka I, Niimura N, Kuroki R, Morimoto Y. Protonation states of buried histidine residues in human deoxyhemoglobin revealed by neutron crystallography. J Am Chem Soc 2007;129(48):14840–14841. [PubMed: 17990881] The first neutron crystal structure (2.1Å resolution) of human deoxyhemoglobin (Hb), one of the larger proteins (64.5 kDa), reveals that both the α-distal and β-distal histidines adopt a positively charged, fully (doubly) protonated form, suggesting their contribution to the T-state Bohr effect of Hb.

17. Kovalevsky AY, Chatake T, Shibayama N, Park SY, Ishikawa T, Mustyakimov M, Fisher SZ, Langan P, Morimoto Y. Preliminary time-of-flight neutron diffraction study of human deoxyhemoglobin. Acta Cryst F 2008;64:270–273.
18. Kinoshita T, Tamada T, Imai K, Kurihara K, Ohhara T, Tada T, Kuroki R. Crystallization of porcine pancreatic elastase and a preliminary neutron diffraction experiment. Acta Cryst F 2007;63:315–317.
19. Langan P, Li X, Hanson BL, Coates L, Mustyakimov M. Synthesis, capillary crystallization and preliminary joint X-ray and neutron crystallographic study of Z-DNA without polyamine at low pH. Acta Cryst F 2006;62:453–456.
20. TeixeiraSCMBlakeleyMPLealRMFMitchellEPForsythVTA preliminary neutron crystallographic study of thaumatin. Acta Cryst F200864: doi: 10.1107/S1744309108008294.
21. Budayova-Spano M, Bonnete F, Ferte N, El Hajji M, Meilleur F, Blakeley MP, Castro B. A preliminary neutron diffraction study of rasburicase, a recombinant urate oxidase enzyme, complexed with 8-azaxanthin. Acta Cryst F 2006;62:306–309.
22. Tanaka I, Kurihara K, Chatake T, Niimura N. A high performance neutron diffractometer for biological crystallography (BIX-3). J Appl Cryst 2002;35:34–40.
23. Kurihara K, Tanaka I, Refai-Muslih M, Ostermann A, Niimura N. A new neutron single crystal diffractometer dedicated for biological macromolecules (BIX-4). J Synchrotron Radiat 2004;11:68–71. [PubMed: 14646137]
24. WilkinsonCBlakeleyMPDauvergneFObservation of the detective quantum efficiency (DQE) and the point spread function (PSF) of the LADI3 diffractometer on the H142 cold guide. ILL internal report2007, ILL07WI02T.
25. Langan P, Mustyakimov M, Fisher Z, Kovalevskyi A, Valone AS, Waltman MJ, Adams PD, Afonine PV, Bennett B, Dealwis C, et al. Protein structures by spallation neutron crystallography. J Synchrotron Radiat 2008;25:215–218. [PubMed: 18421142]
26. Langan P, Greene G, Schoenborn BP. Protein crystallography with spallation neutrons: the user facility at Los Alamos Neutron Science Center. J Appl Crystallogr 2004;37:24–31.
27. Langan P, Greene G. Protein crystallography with spallation neutrons: collecting and processing wavelength-resolved Laue protein data. J Appl Crystallogr 2004;37:253–257.
28. Liu XY, Hanson L, Langan P, Viola RE. The effect of deuteration on protein structure: a high-resolution comparison of hydrogenous and perdeuterated haloalkane dehalogenase. Acta Cryst D 2007;63:1000–1008. [PubMed: 17704569]
29. Budayova-Spano M, Dauvergne F, Audiffren M, Bactivelane T, Cusack S. A methodology and an instrument for the temperature-controlled optimization of crystal growth. Acta Cryst D 2007;63:339–347. [PubMed: 17327671]
30. Arai S, Chatake T, Minezaki Y, Niimura N. Crystallization of a large single crystal of a B-DNA decamer for a neutron diffraction experiment by the phase-diagram technique. Acta Cryst D 2002;58:151–153. [PubMed: 11752796]
31. Chatake T, Mizuno N, Voordouw G, Higuchi Y, Arai S, Tanaka I, Niimura N. Crystallization and preliminary neutron analysis of the dissimilatory sulfite reductase D (DsrD) protein from the sulfate-reducing bacterium *Desulfovibrio vulgaris*. Acta Cryst D 2003;59:2306–2309. [PubMed: 14646103]
32. Maeda M, Chatake T, Tanaka I, Ostermann A, Niimura N. Crystallization of a large single crystal of cubic insulin for neutron protein crystallography. J Synchrotron Radiat 2004;11:41–44. [PubMed: 14646130]
33. Niimura N, Arai S, Kurihara K, Chatake T, Tanaka I, Bau R. Recent results on hydrogen and hydration in biology studied by neutron macromolecular crystallography. Cell Mol Life Sci 2006;63:285–300. [PubMed: 16389451]

NIH-PA Author Manuscript

NIH-PA Author Manuscript

NIH-PA Author Manuscript

34. Brünger AT, Adams PD, Clore GM, DeLano WL, Gros P, Grosse-Kunstleve RW, Jiang JS, Kuszewski J, Nilges M, Pannu NS, et al. Crystallography & NMR system: a new software suite for macromolecular structure determination. Acta Cryst D 1998;54:905–921. [PubMed: 9757107]
35. Bennett BC, Gardberg AS, Blair MD, Dealwis CG. On the determinants of amide backbone exchange in proteins: a neutron crystallographic comparative study. Acta Cryst D 2008;64:764–783. [PubMed: 18566512]
36 •. Weiss KL, Meilleur F, Blakeley MP, Myles DAA. Preliminary neutron crystallographic analysis of selectively CH3-protonated deuterated rubredoxin from Pyrococcus furiosus. Acta Cryst F 2008;64:537–540.Demonstration of selective-labeling protocols that allow the design and production of H/D-labeled macromolecular structures in which the ratio of H to D atoms can be precisely controlled.
37. Hauptman HA, Langs DA. The phase problem in neutron crystallography. Acta Cryst A 2003;59:250–254. [PubMed: 12714776]
38. Teixeira SCM, Zaccai G, Ankner J, Bellissent-Funel MC, Bewley R, Blakeley MP, Callow P, Coates L, Dahint R, Dalgliesh R, et al. New sources and instruments for neutrons in biology. Chem Phys 2008;345:133–151.
39. Schultz AJ, Thiyagarajan P, Hodges JP, Rehm C, Myles DAA, Langan P, Mesecar AD. Conceptual design of a macromolecular neutron diffractometer (MaNDi) for the SNS. J Appl Cryst 2005;38:964–974.
40. Tanaka I, Niimura N, Ozeki T, Ohhara T, Kurihara K, Kusaka K, Morii Y, Aizawa K, Arai M, Kasao T, et al. Neutron biological diffractometer in J-PARC proposed by Ibaraki prefectural government. ICANS-XVII Proceedings 2006, LA-UR-3904, vol III 2006:937–945.
41. Kurihara K, Tanaka I, Chatake T, Adams MWW, Jenny FE Jr, Moiseeva N, Bau R, Niimura N. Neutron crystallographic study on rubredoxin from *Pyrococcus furiosus* by BIX-3, a single-crystal diffractometer for biomacromolecule. Proc Natl Acad Sci U S A 2004;101:11215–11220. [PubMed: 15272083]
42. Ostermann A, Tanaka I, Engler N, Niimura N, Parak FG. Hydrogen and deuterium in myoglobin as seen by a neutron structure determination at 1.5Å resolution. Biophys Chem 2002;95:183–193. [PubMed: 12062378]
43. Chatake T, Kurihara K, Tanaka I, Tsyba I, Bau R, Jenny FE, Adams MWW Jr, Niimura N. A neutron crystallographic analysis of a rubredoxin mutant at 1.6Å resolution. Acta Cryst D 2004;60:1364–1373. [PubMed: 15272158]
44. Chatake T, Tanaka I, Umino H, Arai S, Niimura N. The hydration structure of a Z-DNA hexameric duplex determined by a neutron diffraction technique. Acta Cryst D 2005;61:1088–1099. [PubMed: 16041074]
45. Arai S, Chatake T, Ohhara T, Kurihara K, Tanaka I, Suzuki N, Fujimoto Z, Mizuno H, Niimura N. Complicated water orientations in the minor groove of the B-DNA decamer d(CCATTAATGG)2 observed by neutron diffraction measurements. Nucleic Acids Res 2005;33:3017–3024. [PubMed: 15914673]
46. Ishikawa T, Chatake T, Ohnishi Y, Tanaka I, Kurihara K, Kuroki R, Niimura N. A neutron crystallographic analysis of a cubic insulin at pD 6.6. Chem Phys 2008;345:152–158.
47. Ahmed HU, Blakeley MP, Cianci M, Cruickshank DWJ, Hubbard JA, Helliwell JR. The determination of protonation states in proteins. Acta Cryst D 2007;63:906–922. [PubMed: 17642517]
48. Blakeley MP, Kalb (Gilboa) AJ, Helliwell JR, Myles DAA. The 15-K neutron structure of saccharide-free concanavalin A. Proc Natl Acad Sci U S A 2004;101:16405–16410. [PubMed: 15525703]
49. Coates L, Erskine PT, Wood SP, Myles DAA, Cooper JB. A neutron Laue diffraction study of endothiapepsin: implications for the aspartic proteinase mechanism. Biochemistry 2001;40:13149–13157. [PubMed: 11683623]
50. Li XM, Langan P, Bau R, Tsyba I, Jenney FE, Adams MWW, Schoenborn BP. W3Y single mutant of rubredoxin from *Pyrococcus furiosus*: a preliminary time-of-flight neutron study. Acta Cryst D 2004;60:200–202. [PubMed: 14684930]
51. Sukumar N, Langan P, Jones LH, Thiyagaran P, Schoenborn BP, Davidson VL. A preliminary time-of-flight neutron diffraction study on amicyanin from *Paracoccus denitrificans*. Acta Cryst D 2005;61:640–642. [PubMed: 15858277]

NIH-PA Author Manuscript
NIH-PA Author Manuscript
NIH-PA Author Manuscript

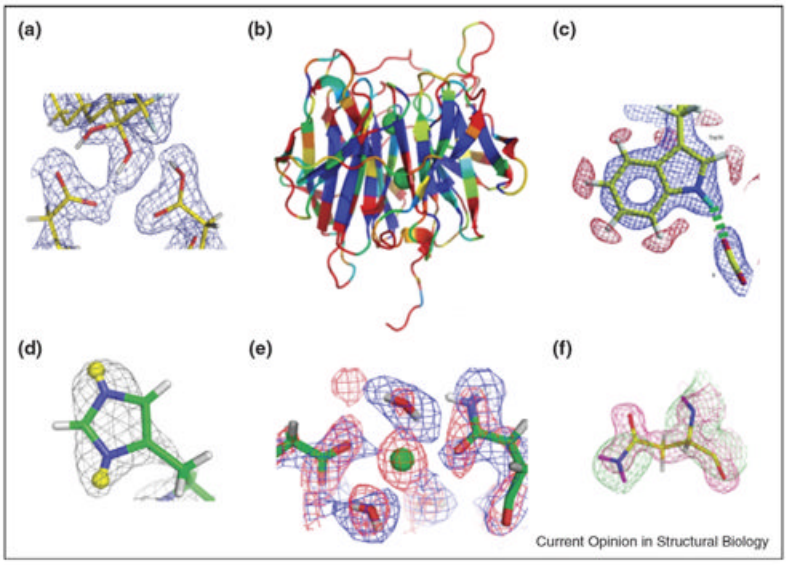

Figure 1.

(a) A *2Fo-Fc* nuclear density map calculated from the joint refined X-ray (1.0Å) and neutron (1.8Å) structure of the enzyme endothiapepsin clearly shows the protonation state of the enzyme and the bound *gem*-diol inhibitor PD-135,040 in the active site [10,11]. **(b)** A topological representation of the extent of H/D exchange at backbone amide groups in the enzyme diisopropyl fluorophosphatase [9•]: blue, nonexchanged; red, fully exchanged. The extent of isotopic exchange is a measure of solvent accessibility and local refolding dynamics. **(c)** A *2Fo-Fc* nuclear density map calculated from the refined 1.6Å neutron structure of a rubredoxin triple mutant, showing a view of residue Trp36. Blue and red contours show positive and negative densities, respectively. The green broken line shows a hydrogen bond between the N—D bond of Trp36 and the carboxyl group of Glu18. Note the positive contours of the N—D group and the entire D_2O molecule, as opposed to the negative contours of the H atoms of the C—H bonds [43]. **(d)** Superimposed *2Fo-Fc* nuclear (green) and electron (red) density maps calculated from the joint refined X-ray (1.1Å) and neutron (2.5Å) structure of photoactive yellow protein, showing residues Asn13. Note the Nδ2 group of Asn13 scatters neutrons more strongly than X-rays and makes the determination of the orientation of Asn side chains much easier and more accurate [16••]. **(e)** Superimposed *2Fo-Fc* nuclear (blue) and electron (red) density maps calculated from the joint refined X-ray (1.8Å) and neutron (2.2Å) structure of enzyme diisopropyl fluorophosphatase, showing the active site. Note that water molecules are clearly oriented in the joint structure [9]. **(f)** A *2Fo-Fc* nuclear density map calculated from the refined 1.8Å neutron structure of the enzyme D-xylose isomerase, showing a view of residue His54. Although the protonation state of this residue is ambiguous in the atomic resolution (0.94Å) X-ray structure, it is clear from the nuclear density that both Nδ1 and Nε2 are protonated [6••].

NIH-PA Author Manuscript
NIH-PA Author Manuscript
NIH-PA Author Manuscript

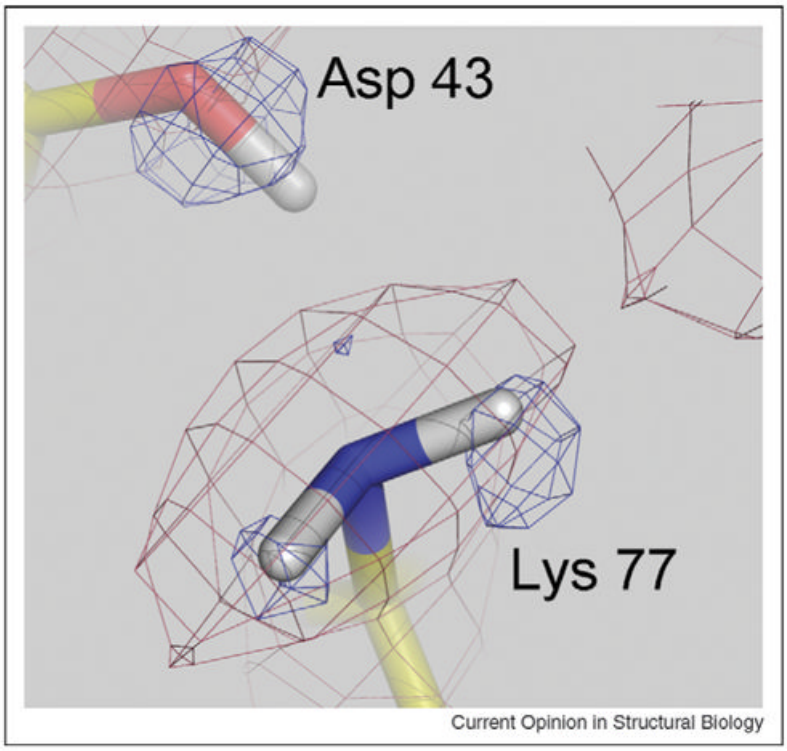

Figure 2.

Superposition of catalytic residues Lys77 and Asp43 from a fully deuterated aldose reductase model (jointly refined against room temperature X + N diffraction data) with a room temperature neutron (2.2Å resolution) *2Fo-Fc* map (magenta contours at 2σ) and a 100 K X-ray high-resolution (0.8Å resolution) *Fo-Fc* map (blue contours at 3σ). Both maps indicate that Lys77 exists in a neutral (doubly protonated) conformation, shown in the model. This neutral conformation, unexpected for a lysine residue hydrogen bonded to an aspartate, led to the proposal of a new catalytic mechanism [4••]. Note that useful neutron diffraction data could be obtained from a crystal with a volume of 0.15 mm^3, radically smaller than usual for neutron diffraction studies.

NIH-PA Author Manuscript NIH-PA Author Manuscript NIH-PA Author Manuscript

Table 1

Recent macromolecular structures solved using NC, with their associated crystallographic and data collection parameters, PDB ID and reference

Name	Lattice constants (Å)/space group	D_{min} (Å)	Crystal volume (mm^3)	Collection time (days)	PDB ID	Reference
BIX-3						
Wild-type rubredoxin (*Pyrococcus furiosus*)	34.3 × 35.3 × 44.2/$P2_12_12_1$	1.5	4.4	35	1vcx	[41]
Met-myoglobin	64.5 × 30.9 × 34.9, β = 105.7°/$P2_1$	1.5	6.3	22	1l2k	[42]
Triple mutant rubredoxin (*Pf*)	34.5 × 35.7 × 43.2/$P2_12_12_1$	1.6	6.0	31	1iu6	[43]
Cubic insulin (pig)	78.9 × 78.9 × 78.9/$I2_13$	2.2	18.0	21	2zpp	[32]
Dissimilatory sulfite reductase D (DsrD)	60.5 × 65.1 × 46.5/$P2_12_12_1$	2.4	1.7	70	1wq2	[31]
Z-DNA d(CGCGCG)	18.5 × 30.8 × 43.2/$P2_12_12_1$	1.8	1.6	70	1vqg	[44]
Elastase/FR130180 complex	51.2 × 57.8 × 75.6/$P2_12_12_1$	2.3	1.6	23	-	[18]
Human deoxyhemoglobin	63.8 × 84.5 × 54.4, β = 99.3°/$P2_1$	2.1	36.0	120	2dxm	[16••]
BIX-4						
B-DNA_d(CCATTAATGG)2	32.9 × 32.9 × 96.1/$P3_221$	3.0	2.8	32	1wqz	[45]
Cubic insulin (p*D* = 6.6)	79.0 × 79.0 × 79.0/$I2_13$	2.7	2.3	21	2efa	[46]
RNase A (PO_4 free)	30.4 × 38.6 × 53.4, β = 105.8°/$P2_1$	1.4	14.0	25	-	D Yagi *et al*. (unpublished)
LADI-I						
Perdeuterated human aldose reductase/ NADP+/IDD-594 complex	50.1 × 67.1 × 47.9, β = 92.4°/$P2_1$	2.2	0.15	93	2r24	[4••]
Concanavalin A	89.4 × 87.3 × 63.1/$I222$	2.2	21.0	15	2yz4	[47]
Concanavalin A at 15 K	89.2 × 86.1 × 61.6/$I222$	2.5	1.6/5.6	34	1xqn	[48]
Rasburicase/8-azaxanthin complex	81.3 × 96.3 × 105.6/$I222$	2.1	1.8	34.5	-	[21]
Endothiapepsin/H261 complex	43.1 × 75.7 × 42.9, β = 97.0°/$P2_1$	2.1	3.5/3.0	69	1gkt	[49]
Xylose isomerase	92.8 × 98.4 × 101.5/$I222$	2.2	4.0	21	-	[7]
W3Y rubredoxin at 15 K (*Pf*)	34.1 × 34.9 × 43.7/$P2_12_12_1$	1.7	1.4	7.5	-	MP Blakeley *et al.* (unpublished)
LADI-III						
Perdeuterated rubredoxin (*Pf*)	33.9 × 34.9 × 43.5/$P2_12_12_1$	1.75	1.4	0.5	-	DAA Myles *et al*. (unpublished)
Perdeuterated rubredoxin (*Pf*)	33.9 × 34.9 × 43.5/$P2_12_12_1$	1.65	4.0	5.5	-	DAA Myles *et al*. (unpublished)
Selectively CH_3-protonated perdeuterated rubredoxin (*Pf*)	33.9 × 34.9 × 43.6/$P2_12_12_1$	1.69	4.1	3.5	-	[36•]
Thaumatin	57.8 × 57.8 × 150.1/$P4_12_12$	2.0	1.4	3.5	-	[20]
Perdeuterated type-III antifreeze protein	32.7 × 39.1 × 46.5/$P2_12_12_1$	2.0	0.13	22	-	I Haertlein *et al.* (unpublished)
Rasburicase/8-azaxanthin complex	80.1 × 96.0 × 105.2/$I222$	1.9	4.0	6	-	M Budayova-Spano *et al.* (unpublished)
A-DNA d(ACCCCGGGT)	32.8 × 32.8 × 78.3/$P4_12_12$	2.3	0.17	4.5	-	R Leal *et al.* (unpublished)
Cytochrome *c* peroxidase	51.6 × 76.7 × 107.2/$P2_12_12_1$	2.4	0.8	5.6	-	P Moody *et al.* (unpublished)
Cex catalytic domain (glycosyl-enzyme intermediate)	87.9 × 87.9 × 80.8/$P4_12_12$	2.5	0.7	8.25	-	L McIntosh *et al.* (unpublished)
PCS						
D-Xylose isomerase	93.9 × 99.7 × 102.9/$I222$	1.8	8.0	19.5	2gve	[6••]
Diisopropyl fluorophosphatase (DFPase)	43.4 × 83.3 × 87.5/$P2_12_12_1$	2.2	0.43	37	-	[9•]
Endothiapepsin/PD-135,040 complex	43.0 × 75.7 × 42.9, β = 97.0°/$P2_1$	1.8	2.7	35	2vs2	[10,11]

NIH-PA Author Manuscript
NIH-PA Author Manuscript
NIH-PA Author Manuscript

Name	Lattice constants (Å)/space group	D_{min} (Å)	Crystal volume (mm^3)	Collection time (days)	PDB ID	Reference
Photoactive yellow protein (PYP)	66.8 × 66.8 × 41, γ = 120°/$P6_3$	2.5	0.79	14	2qws	[15•]
Dihydrofolate reductase/methotrexate complex	93.1 × 93.1 × 73.9, γ = 120°/$P6_1$	2.2	0.3	22.5	2inq	[14••]
Human deoxyhemoglobin	63.8 × 84.5 × 54.4, β = 99.3/$P2_1$	1.8	20	18	-	[17]
Z-DNA d(CGCGCG)	18.0 × 31.2 × 44.9/$P2_12_12_1$	1.6	0.70	18	-	[19]
W3Y rubredoxin	34.32 × 35.31 × 44.23/$P2_12_12_1$	2.1	1.5	4	-	[50]
Amicyanin	a = 28.5, b = 55.9, c = 27.2, β = 95.6/$P2_1$	1.9	2.6	21	-	[51]
D-Xylose isomerase/D-xylulose complex	94.64 × 99.97 × 103.97/$I222$	2.2	8.0	30	3CWH	[8••]

Unpublished results are included to show the trend toward measuring data from smaller crystals.

NIH-PA Author Manuscript
NIH-PA Author Manuscript
NIH-PA Author Manuscript

Table 2

Neutron diffractometers available for protein crystallography

Diffractometer	Method	Flux at sample position (n/(cm^2 s))	Typical crystal size (mm^3)	Cell parameters (Å)	Necessary days to collect data (days)	Resolution (Å)	Power target (spallation source)	Power (reactor)	Responsible
BIX-3 (JAEA)	Monochromatized 2.9 Å	2.9×10^6	>1	<100	>20	>1.4		20 MW	kuroki.ryota@jaea.go.jp
BIX-4 (JAEA)	Monochromatized 2.6 Å	4.5×10^6	>1	<100	>15	>1.4		20 MW	kuroki.ryota@jaea.go.jp
iBIX[a] (J-PARC)	Pulsed white (TOF) 25 Hz (0.7-3.8 Å)	2.1×10^8 at 0.20° divergence	>0.1	<150	>3	>1.2	1 MW Hg target		niimura@mx.ibaraki.ac.jp, i.tanaka@mx.ibaraki.ac.jp
LADI-III (ILL)	Continuous source quasi-Laue (multilayer band-pass filters with $\delta\gamma/\gamma$ = 20% centered at γ = 3.5 Å from 5 to 25%)	3×10^7 using $\delta\gamma/\gamma$ = 20% centered at γ = 3.5 Å	>0.1 (if perdeuterated) >0.5 otherwise	<160	>3	>1.4		58 MW	blakeleym@ill.fr
PCS (LANSCE) [46,47]	Pulsed white (TOF Laue) 20 Hz (0.6-6 Å)	9.7×10^6 at 0.12° divergence	>0.3	<180	>4	>1	0.1 MW W target		langan_paul@lanl.gov
MaNDi[a] (SNS)	Pulsed white (TOF Laue) 60 Hz, adjustable wavelength range with $\Delta\lambda \sim$ 2.7 Å	1.2×10^7 at 0.23° divergence and 6.9×10^7 at 0.56° divergence	>0.1	<150	>1	>1.5	2 MW Hg target		coatesl@sns.g

[a] If under construction.